Brauer, H., "Stromung und warmesuberganb bei rieselfilmen," *VDI-Forshungsheft,* 457 (1956).
Brumfield, L. K., R. N. Houze, and T. G. Theofanous, "Turbulent Mass Transfer at Free Gas-Liquid Interfaces, With Applications to Film Flows," *Intern. J. Heat Mass Transfer,* **18,** 1077 (1975).
Chung, D. K., and A. F. Mills, "Experimental Study of Gas Absorption into Turbulent Falling Films of Water and Ethylene Glycol-Water Mixtures," *Letters Heat Mass Transfer,* **1,** 43 (1974).
Coeuret, F., B. Jamet, and J. J. Ronco, "Transfer de matere aver et sans reaction chimique dans un film tombant cylindrique en regime de transitions et en regime turbulent," *Chem. Eng. Sci.,* **25,** 17 (1970).
Davies, J. T., *Turbulence Phenomena,* Academic Press, New York (1972).
Davis, D. S., and G. S. Crandall, "The Liquid Stationary Film is Gas Absorptions," *J. Am. Chem. Soc.,* **52,** 570 (1930).
Davis, E. J., S. C. Hung, and S. Arciero, "An Analogy for Heat Transfer with Wavy/Stratified Gas-Liquid Flow," *AIChE J.,* **21,** 872 (1975).
Emmert, R. E., and R. L. Pigford, "A Study of Gas Absorption in Falling Liquid Films," *Chem. Eng. Progr.,* **50,** 87 (1954).
Feind, K., "Stromung suntersuchungen bei gegenstrom van rieselfilmen und gas lotrechten rohresn," *VDI-Forshungsheft,* 481 (1960).
Fortescue, G. E., and F. R. A. Pearson, "On Gas Absorption Into a Turbulent Liquid," *Chem. Eng. Sci.,* **22,** 1163 (1967).
Henstock, W. H., "The Effect of a Concurrent Gas Flow on Gas-Liquid Mass Transfer," Ph.D. thesis, Univ. Ill., Urbana (1977).
———, and T. J. Hanratty, "The Interfacial Drag and the Height of the Wall Layer in Annular Flows," *AIChE J.,* **22,** 990 (1976).
Hinze, J. O., *Turbulence,* McGraw-Hill, New York (1959).
Kamei, S., and J. Oishi, "Mass and Heat Transfer in a Falling Liquid Film of Wetted Wall Tower," *Mem. Fac. Eng. Kyoto Univ.,* **17,** 277 (1955).
Kanwisher, J., "On the Exchange of Gases Between the Atmosphere and the Sea," *Deep Sea Research,* **10,** 195 (1963).
Kasturi, G., and J. B. Stepanek, "Two-Phase Flow-IV. Gas and Liquid Side Mass Transfer Coefficients," *Chem. Eng. Sci.,* **29,** 1849 (1974).
King, C. J., "Turbulent Liquid Phase Mass Transfer at a Free Gas-Liquid Interface," *Ind. Eng. Chem. Fundamentals,* **5,** 1 (1966).
Kraus, E. B., "Atmosphere-Ocean Interaction," *Oxford Monographs on Meteorology* (1972).
Lamont, J. C., and D. S. Scott, "An Eddy Cell Model of Mass Transfer into the Surface of a Turbulent Liquid," *AIChE J.,* **16,** 513 (1970).
Lamourelle, A. P., and O. C. Sandall, "Gas Absorption into a Turbulent Liquid, *Chem. Eng. Sci.,* **27,** 1035 (1972).
Levich, V. G., *Physicochemical Hydrodynamics,* Prentice Hall, Englewood Cliffs, N.J. (1962).
Menez, G. D., and D. C. Sandall, "Gas Absorption Accompanied by First-Order Chemical Reaction in Turbulent Jets," *Ind. Eng. Chem. Fundamentals,* **13,** 72 (1974).
Miller, E. G., B. S. thesis, Univ. Del., Newark (1974), cited by Sherwood, T. K., and R. L. Pigford, *Absorption and Extraction,* 2 ed., p. 267, McGraw-Hill, New York (1952).
Miya, M., "Properties of Roll Waves," Ph.D. thesis, Univ. Ill. Urbana (1970).
Nusselt, W., "Die Oberflachenkondensation des Wasserdampfes," *Ver. Deut. Ingr. Z.,* **60,** 549 (1916).
Oliver, D., and T. E. Atherinos, "Mass Transfer to Liquid Films on an Inclined Plane," *Chem. Eng. Sci.,* **23,** 525 (1968).
Schlichting, H., *Boundary-Layer Theory,* McGraw-Hill, New York (1968).
Son, J. S., and T. J. Hanratty, "Limiting Relation for the Eddy Diffusivity Close to a Wall, *AIChE J.,* **13,** 689 (1967).
Stirba, C., and D. M. Hurt, "Turbulence in Falling Liquid Films," *ibid.,* **1,** 178 (1955).
Telles, A. S., and A. E. Dukler, "Statistical Characteristics of Thin, Vertical, Wavy, Liquid Films," *Ind. Eng. Chem. Fundamentals,* **9,** 412 (1970).
Vyazovov V., "A Theory of Absorption of Weakly Dissoluble Gases by Liquid Films," *J. Tech. Phys. (U.S.S.R.),* **10,** 1519 (1940).

Manuscript received June 2, 1977; revision received May 30, and accepted September 6, 1978.

Residence Time Distributions of Paper Pulp Slurries in Vertical Laminar Flow

R. M. MOREIRA
and
R. M. FELDER

Department of Chemical Engineering
North Carolina State University
Raleigh, North Carolina 27650

The hydrodynamic behavior of paper pulp slurries in vertical laminar flow has been observed and modeled. Radiotracers were used to tag both the liquid and solid phases of slurries flowing in 4 and 30 cm pipes. Residence time distributions were determined for each phase and were used to derive and compare several flow models. A model consisting of a central core in plug flow circumscribed by a clear Newtonian annulus provides a good representation of the observed slurry behavior. Correlations between the model parameters and the Reynolds number and slurry consistency are presented, and implications of the results on the design of slurry flow reactors are discussed.

SCOPE

Modeling a slurry flow reactor involves the direct or indirect specification of the residence time distribution of the solid phase. Under different conditions, the slurry may be treated either as a homogeneous or a heterogeneous fluid; when the solid and liquid phases move together, the slurry can be dealt with as a single non-Newtonian liquid, while if slip occurs, the existence of separate phases must be explicitly taken into account.

The observation of a slurry flow using tracers is one way to determine how closely heterogeneous and homogeneous models approximate reality. Flow patterns can be observed by means of residence time distribution measurements; however, since the behavior of the phases may be different, each phase must be tagged separately.

Correspondence concerning this paper should be sent to R. M. Felder. R. M. Moreira is at the Instituto de Pesquisas Radioátivas, Belo Horizonte, Brazil.

0001-1541-79-2123-0131 $01.45.

In this study, the hydrodynamic behavior of a paper pulp slurry in vertical laminar flow was investigated in a series of static settling experiments and dynamic tracer response measurements. Radiotracers were used to tag both the liquid and solid phases of slurries flowing in a 4 cm ID pipe and a 30 cm ID tower. Impulse responses obtained at the inlet and outlet of test sections were deconvoluted by Fourier analysis to determine solid and liquid phase residence time distributions, and the resulting distributions were, in turn, used to test and compare various models for slurry flow. The models tested include a pseudo-homogeneous power law model, a dispersion model, and a two-phase model consisting of a central core in plug flow and a clear laminar annulus.

CONCLUSIONS AND SIGNIFICANCE

Of the models tested, the one that provides the best combination of simplicity and correspondence with observed slurry behavior is a clear annulus model with interphase slip. The lisuid velocity profile consists of a central core in plug flow circumscribed by a Newtonian annulus, and suspended solids are contained within the core and move with a velocity less than that of the core liquid. The core diameter approaches the flow channel diameter as the Reynolds number decreases and the weight fraction of suspended solids increases. Although some axial dispersion is observed in the measured solid phase residence time distributions, the assumption of ideal plug flow for this phase appears justified, even for slurry consistencies of 0.1% solids and less.

The results of the measurements have been used to derive dimensionless correlations for estimating the parameters of this model. A combination of Darcy's law, the Kozeny-Carman equation, and a modified Labrecque correlation allows an accurate prediction of the interphase slip velocity in static settling experiments, but underpredicts the slip velocity in dynamic measurements. Even with this error, the model provides estimates of the mean residence time that are substantially closer to the measured values than are estimates obtained with a simple homogeneous ideal plug flow model.

BACKGROUND

The hydrodynamic behavior of rodlike particles has been studied by Mason and Manley (1952), whose investigations showed that an isolated fiber under shear flow rotates about an axis and therefore sweeps out a region greatly in excess of its own volume. This phenomenon causes the occurrence of multiple particle interactions when the consistency of the suspension is above a critical level whose magnitude is usually low, and accounts for the ability of small quantities of suspended particles to cause substantial modifications in flow patterns.

Existing studies of pulp slurry flow have involved measuring friction losses as functions of pulp and flow channel properties (Brecht and Heller, 1950; Daily and Bugliarello, 1959). These studies show that in the laminar flow regime, the slurry friction factors are higher than the friction factor of pure water, while in the turbulent regime, the situation is reversed and the fiber suspensions are drag reducing. Moreover, the transition between regimes occurs at higher Reynolds numbers for slurries than for pure water.

An investigation of slurry flow characteristics was carried out in the period 1956 to 1965 at the Massachusetts Institute of Technology. A brief summary of the resulting papers and reports has been published by Robertson (1965). In the first of these studies, Daily and Bugliarello (1959) pointed out that fiber suspensions do not behave as Newtonian fluids and that attempts to represent them by common non-Newtonian models were generally unsuccessful. In a subsequent publication, Bugliarello and Daily (1961) attributed this result to phase segregation and slip in flowing suspensions. Pseudoplastic and Bingham plastic models failed because they could not predict the experimentally measured values of the wall shear stress. A comparison between experimental and calculated velocity profiles was not attempted by these authors, nor was any indication given of the magnitude of the disparity between the model predictions and the experimental data.

Many researchers have observed phase segregation phenomena in different regimes of flow. Forgacs et al. (1958) established that in laminar flow of fiber suspensions in pipes, a central region containing all of the fibers is surrounded by a clear liquid annulus; the core moves at a uniform velocity and occupies the greatest part of the pipe cross section, and the shear and velocity variations occur primarily in the annulus. Some authors, like Moller et al. (1971), believe that the velocity profile in the annulus is parabolic, while others, like Bugliarello and Daily (1961), consider the profile to be essentially linear (Couette flow). The annulus thickness has been observed to increase with increasing flow rate and to decrease with increasing fiber concentration. As the flow velocity is increased, a value is reached at which the flow in the annulus becomes unstable and the outer walls of the plug begin to erode, and as the velocity increases further, the boundaries of the core gradually recede toward the center of the pipe. This is the transition regime. Eventually, a velocity is reached at which the central plug completely vanishes. The flow is then turbulent over the entire pipe cross section, and there is no sharp phase segregation.

The clear annulus model is based on visually observed phenomena and has provided a basis for useful data correlations, but Wrist (1967) notes that some of its features still require explanation. While the fiber network yield stress (which is far from trivial to measure) is recognized as the factor that governs the behavior at the wall of the plug and consequently determines the flow regime, the manner in which it does so is not yet understood. Thus, although existing models successfully correlate the annulus thickness with the shear at the wall of the network and with the fiber concentration, the models are not capable of predicting flow behavior from first principles. Neverthe-

less, attempts have been made to use the clear annulus model for design (Moller et al., 1971; Stenuf and Anumolu, 1972; Moller and Duffy, 1974). The inherent limitations of the proposed methods have been discussed by these authors.

Some velocity profile measurements, restricted to the turbulent regime, have been made by Daily and Bugliarello (1961), Mih and Parker (1967), and Sanders and Meyer (1971), who observed profiles blunter than those corresponding to pure water. Specifically designed and rather elaborate probes are required to avoid plugging by the fibers when such measurements are made.

Transport theory provides the general foundation for analyzing systems involving two phase flow. When neither heat nor mass transfer occurs and the only body force acting on the mixture is gravity, the description of the state of the system is accomplished by the momentum balance and continuity equations (Broadkey, 1967). A comprehensive analysis of solid-liquid flow along these lines is given by Zuber (1964), who developed a model that could be used to describe operations ranging from sedimentation to fluidization and diffusion of kinematic waves. Zuber's analysis was restricted to dispersed phases consisting of geometrically well-defined particles and to the laminar regime, but the possibility of extension to the turbulent range was discussed.

Letan (1974) extended Zuber's work to the range of intermediate particle Reynolds numbers and performed tests on slurries with complex particle shapes, obtaining a good agreement with the theory. Researchers in paper pulp technology have also used the momentum balance approach; apparently unaware of Zuber's work, however, they imposed relatively restrictive assumptions in their analyses (Nelson, 1964; Emmons, 1965; Han, 1965; Sanders and Meyer, 1971). In his paper, Emmons stresses the assumption of continuum properties for both phases, which, while not exact for the dispersed phase on a microscopic scale, can be tolerated for practical purposes in the case of moderately concentrated mixtures. The further development of this theory may ultimately provide a suitable model for the flow dynamics of pulp suspensions.

The influence of the non-Newtonian nature of suspensions on the distribution of residence times in flow systems has occupied the attention of some researchers, most of whom had in mind applications to polymer dispersions. Thus, Fan and Hwang (1965) extended Taylor's theory of dispersion in laminar flow to power law fluids, and Novosad and Ulbrecht (1965) and Wein and Ulbrecht (1972) extended the analysis to other types of non-Newtonian fluids using an analytical technique for residence time distribution prediction introduced by Bosworth (1948). This subject has recently been reviewed by Wen and Fan (1975) and Osborne (1975). Experimental measurements of residence time distributions for Newtonian fluids in laminar flow have been reported by Sheppard et al. (1959), Beek et al. (1967), and Gardner et al. (1973).

MODELS FOR LAMINAR SLURRY FLOW

The most accurate approach to modeling slurries in laminar flow involves writing and solving coupled equations of continuity and motion for each phase (see, for example, Zuber, 1964). Such models are difficult to apply, however. At best they require a considerable degree of empiricism, and they are particularly ill suited to represent the behavior of paper pulp slurries, whose geometrical properties are almost impossible to characterize with any degree of precision.

Two simplified models are described in the paragraphs that follow: a pseudo homogeneous power law model and a two phase flow model consisting of a clear laminar annulus and a core containing all of the particles and moving in plug flow.

Pseudo Homogeneous Model (Metzner, 1956)

Let us suppose that a slurry moves through a cylindrical flow channel of radius R_t and length L with a velocity $u(r)$.

Novosad and Ulbrecht (1965) and Wein and Ulbrecht (1972) have derived hydrodynamic relations for purely convective laminar flow of power law fluids in circular ducts. The basis of the model is the power law model equation of state for the shear stress τ_{rz}:

$$\tau_{rz} = -m\left[\frac{du}{dr}\right]^n \tag{1}$$

From this equation can be derived the expressions for the velocity profile

$$u(r) = u_m\left[1 - \left(\frac{r}{R_t}\right)^{1+1/n}\right] \tag{2}$$

the relationship between the mean and maximum velocities (and hence between the mean residence time and the breakthrough time)

$$u_m = \frac{3n+1}{n+1}\,\bar{u} \tag{3}$$

$$t_o = \frac{n+1}{3n+1}\,\bar{t} \tag{4}$$

and expressions for the residence time distribution

$$E(t) = \frac{2n\bar{t}^{\,2}}{(3n+1)\,t^3}\left[1 - \frac{(n-1)\,\bar{t}}{(3n+1)\,t}\right]^{\frac{n-1}{n+1}} H\left\{t - \frac{(n+1)\,\bar{t}}{3n+1}\right\} \tag{5}$$

and its Laplace transform

$$G(s) = \frac{2\sqrt{st_o}}{t_o}\exp(-st_o/2)\,\Gamma(1-\nu)\,W \tag{6}$$

In these equations, $\nu = (n+1)/(n-1)$, and W satisfies Whittaker's equation:

$$\frac{d^2W}{d(st_o)^2} + \left[-\frac{1}{4} + \frac{\nu - 1.5}{st_o} - \frac{3}{4(st_o)^2}\right]W = 0 \tag{7}$$

Clear Annulus Model with Interphase Slip

The clear annulus model is described in part by the equations for the liquid phase shear stress:

$$\tau_{rz} = -\mu\frac{du}{dr}, \quad r \geq R_c \tag{8a}$$

$$\tau_{rz} = \tau_o, \quad r < R_c \tag{8b}$$

If ψ is the ratio R_c/R_t, then the following quantities can be derived from the constitutive Equations (8): the liquid phase velocity profile

$$u_l(r) = u_{lm}\frac{[1 - (r/R_t)^2]}{(1-\psi^2)}, \quad r \geq R_c \tag{9a}$$

$$\equiv u_{lm} \qquad r < R_c \tag{9b}$$

the maximum velocity and breakthrough time

$$u_{lm} = \frac{2}{(1+\psi^2)}\overline{u} \tag{10}$$

$$t_o = \frac{(1+\psi^2)}{2}\overline{t} \tag{11}$$

the liquid phase residence time distribution

$$E_l(t) = \frac{2\psi^2}{1+\psi^2}\delta(t-t_o) + \frac{2t_o^2}{t^3}\left(\frac{1-\psi^2}{1+\psi^2}\right)H(t-t_o) \tag{12}$$

and its Laplace transform,

$$G(s) = \frac{2\psi^2}{1+\psi^2}e^{-st_o} + 2\left(\frac{1-\psi^2}{1+\psi^2}\right)E_i(st_o), \qquad Re(st_o) > 0 \tag{13}$$

The solid phase is assumed to be distributed uniformly across the central core of radius R_c and to move with a velocity

$$u_s = u_{lm} - u_{\text{slip}} \tag{14}$$

A hydrodynamic analysis along lines suggested by Zuber (1964) is used to arrive at an expression for the slip velocity u_{slip}. If the flow is isothermal, if interphase mass transfer is neglected, and if the only body force acting on the system is gravity, the system can be completely defined by the equation of continuity of the liquid phase

$$\frac{\partial}{\partial t}(\epsilon\rho_l) = -\nabla\cdot\rho_l u_l \tag{15}$$

the equation of continuity of the solid phase

$$\frac{\partial}{\partial t}[(1-\epsilon)\rho_s] = -\nabla\cdot(1-\epsilon)\rho_s u_s \tag{16}$$

and the momentum balance equation for the two-phase suspension:

$$\epsilon\rho_l\frac{Du_l}{Dt} + (1-\epsilon)\rho_s\frac{Du_s}{Dt} = -\nabla\cdot\tau - \nabla p - g[\epsilon\rho_l + (1-\epsilon)\rho_s] \tag{17}$$

The operator $D(\ )/Dt$ stands for the substantial derivative as defined by Bird et al. (1965). For steady state vertical flow, uniform voidage, incompressible phases, a constant circular cross section, and negligible friction at the wall, Equations (15) to (17) yield

$$\frac{dp}{dz} = -g[\epsilon\rho_l + (1-\epsilon)\rho_s] \tag{18}$$

Determining the relative motion of the two phases requires the use of the drag equation. Since Zuber developed this equation for the case in which solid phase consisted of spherical particles, we will simply state it in its general form for a particle in unidimensional flow:

$$F - V\frac{dp}{dz} - V\rho_s g = 0 \tag{19}$$

The three terms on the left-hand side of Equation (19) are, respectively, the forces due to viscous drag, the pressure gradient in the liquid surrounding the particle, and the force of gravity. Beginning with this system of equations, Zuber arrived at models of various unit operations by using the boundary conditions appropriate to each case. It is important to notice that there is no need to assume equal phase velocities, a restrictive assumption frequently made in the literature.

Before this system of equations can be solved, some expression must be substituted for the drag force F in Equation (19). When pulp slurries are involved, the difficulty is that the irregular shape of the fibers precludes the use of established correlations for simple particle geometries. What may be done instead is to average the interphase forces over a gross volume element and to account for the drag force using Darcy's law (Emmons, 1965; Sanders and Meyer, 1971):

$$\overline{F} = \mu\epsilon\, u_{\text{slip}}/K \tag{20}$$

If this equation is used, the apparent viscosity of the suspension is not required explicitly; all viscous effects are lumped in the permeability.

If Equation (19) is averaged over a unit volume element and Equation (20) is used to replace $\overline{F}$, and if the pressure gradient dp/dz is eliminated using Equation (18), the following expression for the slip velocity is obtained:

$$u_{\text{slip}} = \frac{(1-\epsilon)(\rho_s-\rho_l)Kg}{\mu} \tag{21}$$

The Kozeny-Carman equation, which is widely used in the analysis of fluid permeation through porous media, relates the permeability to the mean particle surface-to-volume ratio S_p

$$\frac{1}{K} = \frac{k(1-\epsilon)^2 S_p^2}{\epsilon^3} \tag{22}$$

so that Equation (21) becomes

$$u_{\text{slip}} = \frac{\epsilon^3(\rho_s-\rho_l)\,g}{\mu(1-\epsilon)\,S_p^2\,k} \tag{23}$$

A value of $k = 5.55$ was found by Robertson and Mason (1949) to provide excellent data correlations for suspensions of cotton, rayon, wood, and glass wool fibers. For fibrous particles, Carroll's correlation for k is commonly used (Han, 1965, 1969; Sanders and Meyer, 1971):

$$k = 5.0 + \exp[14(\epsilon - 0.80)] \tag{24}$$

This correlation was obtained in tests with relatively stiff nylon fibers of circular cross section. Subsequently, Labrecque (1968) worked with more flexible and deformable nylon fibers and took into account the decrease in exposed fiber surfaces caused by these properties. He found that the Kozeny factor could be correlated with both porosity and fiber cross-section deformation by quadratic expressions of the form

$$k = \sum_{n=0}^{n}(a_n + b_n\epsilon + c_n\epsilon^2)\,A_r^n \tag{25}$$

where the coefficients a_n, b_n, c_n are determined by curve fitting. The term A_r is the aspect ratio, that is, the ratio between the largest and the smallest dimension of the deformed fiber cross section.

All of the terms on the right-hand side of Equation (21) for the slip velocity u_{slip} can now be evaluated. The voidage ϵ can be calculated from the fiber density and concentration, the Kozeny factor k can be estimated from Equation (24) or (25), and the other terms are measurable experimental parameters and physical properties. Thus, if the slip velocity could be independently determined, it would provide a check on the correctness of the original model and of the simplifying assumptions in the derivation of Equation (21). Tracer experiments can provide the necessary data for this determination.

EXPERIMENTAL EQUIPMENT AND PROCEDURES

Measurement of Pulp Properties

To test the flow models to be outlined, it was necessary to measure the specific volume of the pulp fibers, a determination complicated by the fact that the fibers swell as they absorb water. A method developed by Robertson and Mason (1949) and tested by Cowan (1970) and Schweitzer (1975) was used for this purpose.

In the Robertson-Mason experiment, a fiber pad is placed in a plunger-fitted glass cylinder. The cell base and the flat portion of the plunger are perforated and covered with copper screens. The bed depth and pressure head are measured by means of cathetometers, with the pressure head being given by the difference between the upper level of the liquid in the permeability tube and the lower level in a side arm.

Air bubbles are first eliminated from the fiber mat by successive boiling and vacuum desiccation cycles. The permeation rate of water through the mat is then measured and substituted in Darcy's law to calculate the permeability

$$K = \frac{Q\mu L}{A\Delta p} \tag{26}$$

The values of the permeability determined in this manner may be correlated using the Kozeny-Carman equation, Equation (22). One of the quantities in this equation, the void fraction of the swollen fibers, is related to the mass concentration of fibers in the suspension by

$$\epsilon = 1 - \overline{V}c \tag{27}$$

Another parameter of the Kozeny-Carman equation, the surface-to-volume ratio of the swollen fibers, is

$$S_p = \sigma/\overline{V} \tag{28}$$

Substituting these expressions for ϵ and S_p in Equation (22) and setting $k = 5.55$,* we get

$$(Kc^2)^{1/3} = (5.55\,\sigma^2)^{-1/3}\,(1 - \overline{V}c) \tag{29}$$

If permeabilities are measured at several different concentrations, a plot of $(Kc^2)^{1/3}$ vs. c should, from Equation (29), yield a straight line, provided that conditions are such that the Kozeny-Carman equation applies. The specific surface area σ and the effective specific volume $\overline{V}$ may then be determined from the slope and intercept.

This method was first tested with nonswelling Dacron fibers of known specific volume, and agreement to within 3% was obtained. The specific volume and surface area of the unbleached kraft pulp fibers used in the present study were then determined to be $\overline{V} = 3.15$ cm^3/g and $\sigma = 5\,740$ cm^2/g. The plot from which these figures were derived is shown in Figure 1.

The determination of ρ_f, the density of the dry pulp fibers (nonswollen basis), was made by pycnometry using a method described by Stamm (1929). A value of 1.57 g/cm^3 was obtained. The apparent density of the wet fiber was next calculated from the dry fiber density and the specific volume of the wet fibers by the formula

$$\rho_s = \rho_l - \frac{\rho_l - \rho_f}{\overline{V}\,\rho_f} \tag{30}$$

Substitution of the previously calculated values of ρ_f and $\overline{V}$ in the right-hand side of Equation (30) yielded $\rho_s = 1.12$ g/cm^3.

* For the given experimental conditions, this empirical value found by Robertson and Mason (1949) was quite close to values predicted by Equations (24) and (25).

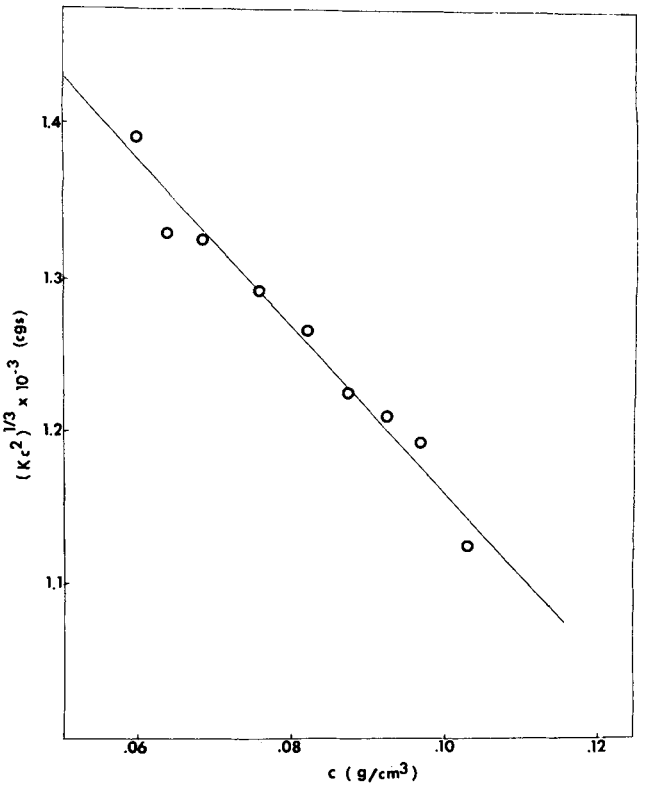

Fig. 1. Kozeny-Carman plot of settling data.

Slurry Flow System

Slurries of an unbleached softwood kraft pulp in water were pumped through a straight vertical 4.074 cm diameter steel pipe. To obtain laminar flow conditions, a calming section of 2.60 m preceded the test section of 1.89 m. The slurry flowed into and out of the pipe through flexible rubber tubes with matching diameters and no sharp bends.

A second, larger unit was also used, which consisted of a steel tower 0.305 m in diameter by 0.914 m high. The slurry entered the tower through a 5 cm opening in the wall at a point 7.6 cm above the bottom of the tower, and the effluent emerged by overflow into a tray circumscribing the outer perimeter of the tower. A schematic of the flow circuit is shown in Figure 2.

Suspensions of pulp were prepared at their desired consistencies in a 1 200 l stirred wooden tank. The slurry was propelled through the circuit by means of a 3/4 kW centrifugal pump and was either recirculated through the mixing tank or allowed to flow through the pipe or tower. In the last two cases, the outflow was collected in a 1 200 l steel holding tank, in which radiotracers were allowed to decay.

The inlet lines to the pipe and tower each contained tees with rubber septa for tracer injections. The injection point for the pipe was located in the inlet section, and that for the tower was situated 0.8 m from the inlet. Scintillation detectors were placed at both extremities of the pipe test section and 0.305 m above the inlet and 0.305 m below the outlet of the tower. The probes consisted of 3.2 cm crystals and photomultiplier bases and a photomultiplier-preamplifier unit. The counting chain consisted of an amplifier, timer-scalar with buffer memory, high voltage power supply, printout control module, and digital printer.

The low flow rates required for laminar flow conditions in the pipe were obtained with the arrangement of piping and valves shown in Figure 2. Flow control by throttling

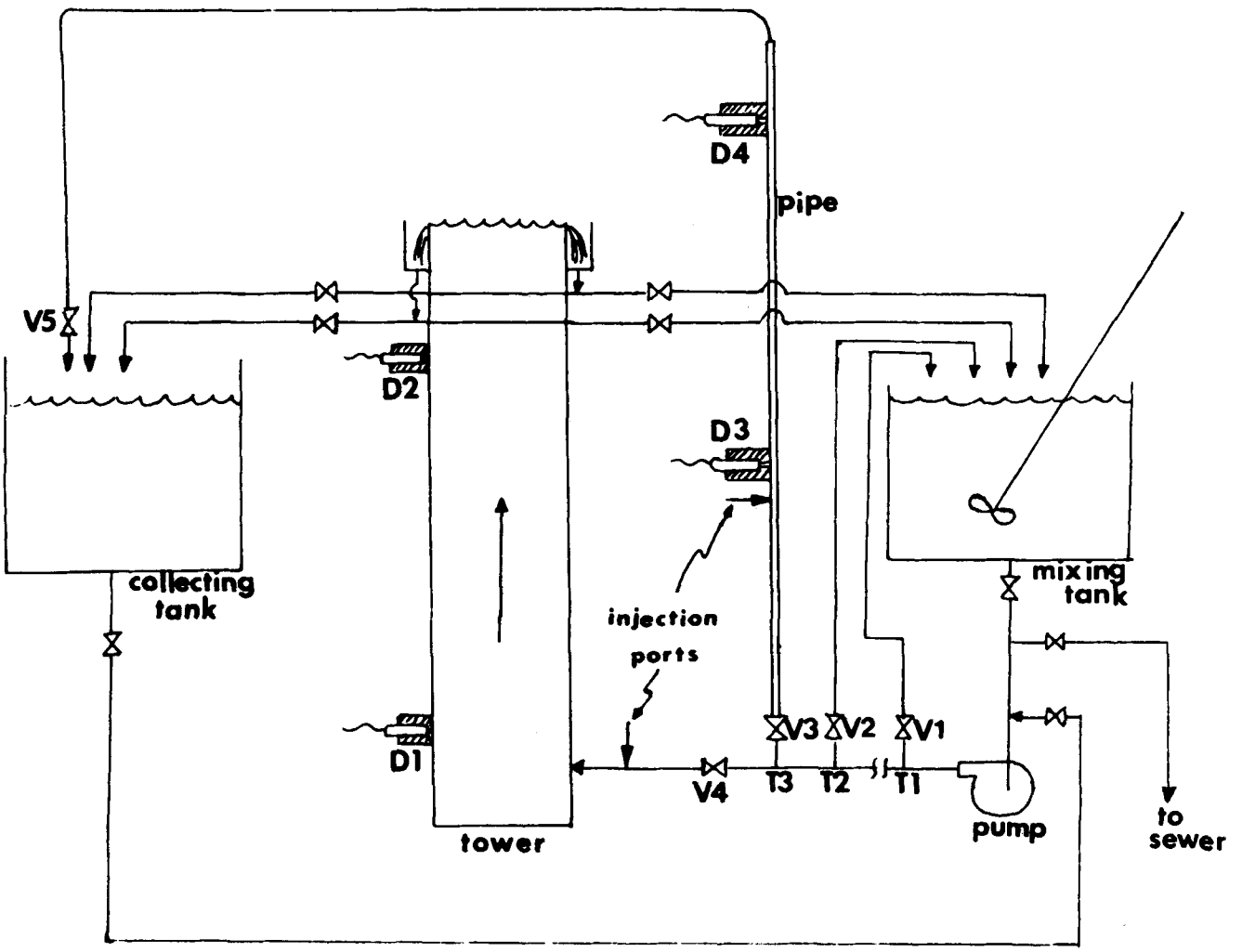

Fig. 2. Flow circuit.

valve V5 was inefficient, particularly when concentrated suspensions were used, because the required slight opening caused accumulation of fibers upstream of the valve with attendant flow rate reductions. Partial opening of valves V1 and V5 also did not work because the slow flow in the rather long horizontal line from T1 to T3 caused fiber deposition. Addition of a second recycle line at T2 and a combination of openings of valves V1, V2, V3, and V5 allowed the attainment of steady flow rates throughout the duration of the tests.

Tracers

The liquid phase tracer chosen was Mn^{56} in the form of a 50% manganous nitrate solution. Manganese was convenient for its hard gamma radiation (up to 2.98 Mev), brief half life (2.6 hr), and solubility.

The selection of a tracer for the pulp was a more difficult problem. In an initial test, pulp was irradiated in a nuclear reactor, and the activity decay pattern was observed. The data revealed the existence of manganese in the material, but in an amount too small to provide an adequate specific activity. A literature search showed that the following radiotracers had been used for pulp tagging: I^{131} by Sankey et al. (1951), Ba^{140} by Fogelberg and Johanson (1958), Cu^{64} and Ca^{140} by Chatters and Petterson (1967), Ir^{194} by Fogelberg and Johanson (1958) and Chatters and Petterson (1969), and Au^{198} by Balla et al. (1971). These isotopes were also unsuitable for the present study. Those which did not have excessively long half lives could not be adsorbed in sufficient quantities to provide an adequate specific activity.

Fiber tracing experiments can be performed using irradiated glass fibers as tracers. This procedure, which is described by Ljunggren (1968), can give reliable results if the suspension contains more than 0.5% solids by weight. Sodium, one of the main components of glass, yields the radioisotope Na^{24} (2.75 Mev gammas, 15 hr half life) which is suitable for the purposes of this study. An insulating glass wool was accordingly chosen to be used as a solid phase tracer. The glass fibers were reduced in size to make them compatible with the pulp fibers and were washed thoroughly prior to irradiation to remove weakly bound activatable species.

Procedure for Tracer Response Measurements

Prior to the runs, the tracers were activated in the North Carolina State University Pulstar reactor. Two milliliters of the liquid manganese solution and 2 mg of glass fibers were doubly encapsulated in polyethylene vials, heat sealed, and irradiated. Prior to the encapsulation, the fibers were vigorously agitated to avoid the presence of lumps that might clog the injector; they were then filtered, washed, and encapsulated in a moist state to facilitate dispersion immediately before injection. The manganese solution was irradiated for 10 min at a flux of 10^{11} neutrons/$cm^2 \cdot s$ to produce an estimated activity of 8 mCi of Mn^{56}, and the glass fibers were irradiated for 30 min at 10^{13} neutrons/$cm^2 \cdot s$ to produce an estimated activity of 2 mCi of Na^{24}. The radioactive material was transported to the site of the experiment inside lead shieldings, and the required manipulations were performed as quickly as possible behind lead bricks. The glass fibers were redispersed

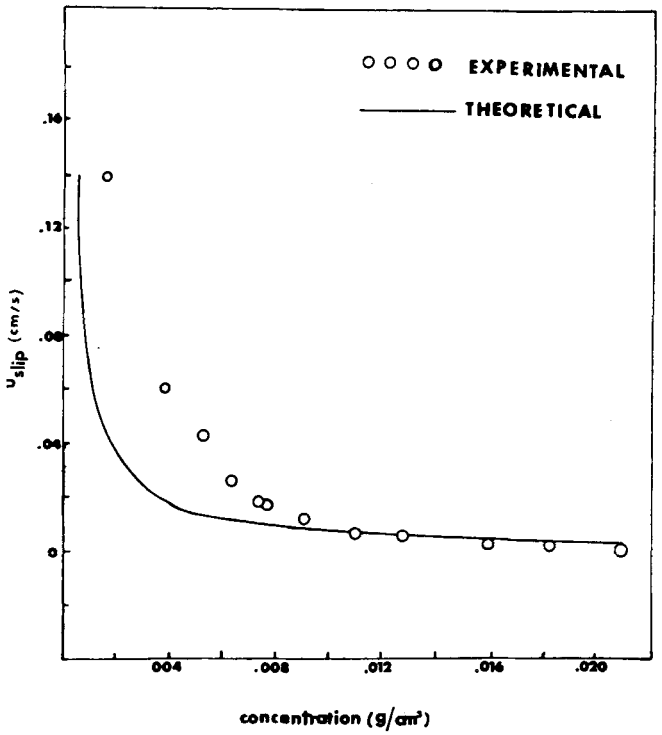

Fig. 3. Settling velocities: Carroll's correlation for Kozeny factor.

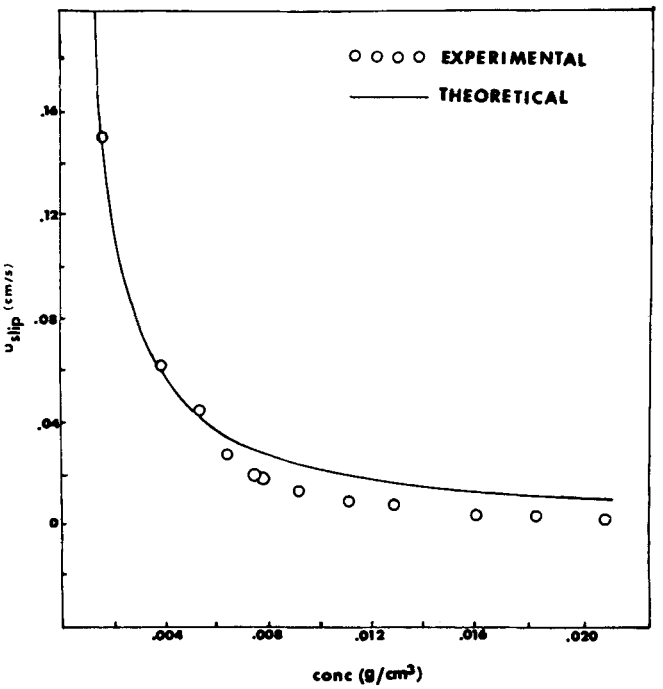

Fig. 4. Settling velocities: Labrecque correlation for Kozeny factor.

in water, and the manganese tracer solution was mixed with an approximately equal volume of inactive solution which served as a carrier. Both tracers were injected by means of syringes with 13 gauge needles 9 cm long, so that the tip could be positioned at the flow axis. The duration of the injection was less than 1 s.

The slurry was circulated through the system for some time before injection to insure homogeneity, and the background count rate was taken during this period. Immediately before injection, a sample was withdrawn for tracer concentration measurement, and the recycle line was closed so that all of the outflow was directed to the collecting tank.

Data Reduction

The tracer response data were first corrected for background and activity decay. When the input and output peaks overlapped, resolution was achieved by logarithmic extrapolation of the input peak tail using the last ten to twenty-five unambiguously defined points of the peak.

The conditions of the experiment were taken to be such that uniform injection-uniform detection formulas could be applied to the determination of the residence time distribution (Levenspiel and Turner, 1970; Levenspiel, Lai, and Chatlynne, 1970; Gardner et al., 1973). The measured impulse responses $C(t)$ were first normalized by the formula

$$C_n(t) = \frac{t^{-2} C(t)}{\int_o^\infty t^{-2} C(t)\, dt} \qquad (31)$$

System residence time distributions were then calculated using one of two methods. In the first, Fourier transforms of the input and output residence time distributions were calculated using a fast Fourier transform algorithm suggested for real-valued functions by Brigham (1974). The substantial scatter in the tails of the responses necessitated filtering the peaks; a Hamming window was applied for this purpose (Ackroyd, 1973). The filtered transforms were truncated at the frequency for which the amplitude was one twentieth of its zero frequency value. The Fourier transform of the system residence time distribution (the system transfer function) was calculated as the quotient of the output and input peak transforms, and the distribution itself was obtained by inverting the transform, again using the fast Fourier transform algorithm.

Model parameters were initially determined by applying nonlinear regression in the time domain using the deconvoluted impulse responses (Harrison, Felder, and Rousseau, 1974). The results offered little improvement over simpler methods based on moment differences and peak maximum lags, however, and so the latter methods were used throughout most of the study.

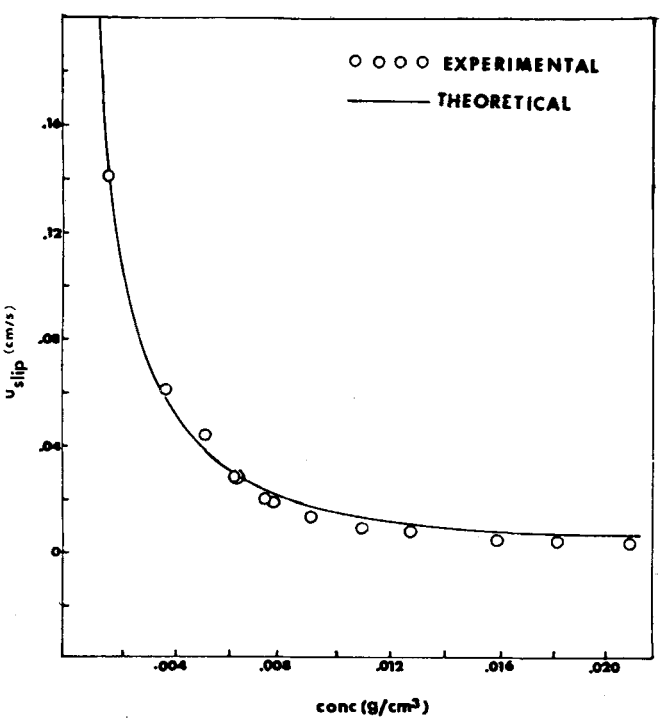

Fig. 5. Settling velocities: Modified Labrecque correlation for Kozeny factor.

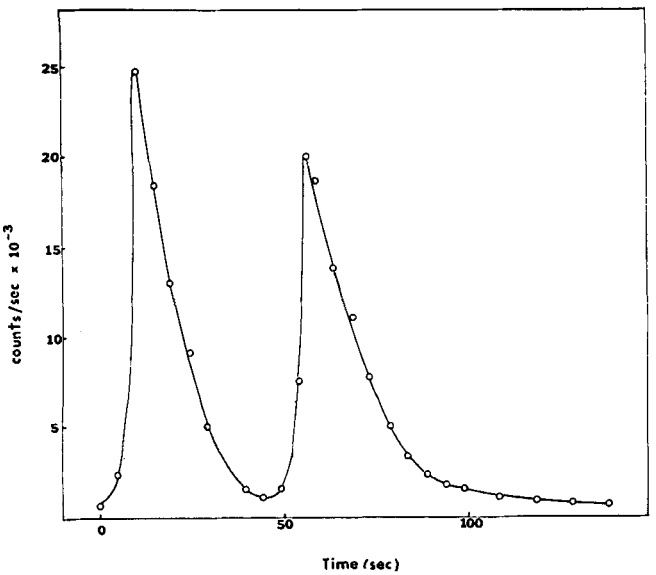

Fig. 6. Representative tracer response: liquid phase tagging.

EXPERIMENTAL RESULTS

Static Settling Experiments

The two phase flow models to be tested contain at least one parameter (k) that must be specified empirically; moreover, the applicability of a model to a particular solid phase cannot be known in advance, and should deviations occur between experimental and predicted responses, the origin of the deviations could be experimental, theoretical, or both.

To clarify this point, a test of the model was performed under conditions more controlled than those which would be encountered in the dynamic response tests. Suspensions of the kraft pulp were stirred into near uniformity in a 2 000 ml beaker and were allowed to settle. The rate of settling was measured by timing the descent of the upper layer of the slurry during the initial stages of the process, before fiber interactions introduced a hindrance to settling.

Figure 3 shows a plot of the settling velocity vs. the slurry concentration, along with the curve predicted by Darcy's law and the Kozeny-Carman equation, Equation (22), with Carroll's correlation, Equation (24), being used to predict the Kozeny factor k. An indication of the goodness of the fit is the value of the correlation coefficient

$$R = 1 - \frac{\sum_{i=1}^{N} [v_{si} - v_s(c_i)]^2}{\sum_{i=1}^{N} [v_{si} - v_s]^2} \qquad (32)$$

For the curve of Figure 3, $R = 0.38$, where $R = 1.0$ would represent a perfect fit.

Carroll's correlation originated from results of tests on filtration through glass fibers, which are rigid relative to paper pulp fibers, whereas Labrecque's correlation, Equation (25), was developed for more flexible fibers and allowed for fiber contact and deformation. A comparison of experimental settling velocities with the values predicted by the Kozeny-Carman equation with Labrecque's correlation for the Kozeny factor is shown in Figure 4, with the aspect ratio (ratio between largest and smallest dimensions of the fiber cross section) set equal to one, corresponding to cylindrical fibers. The values of the empirical parameters in the correlation are those used by Labrecque (1968).

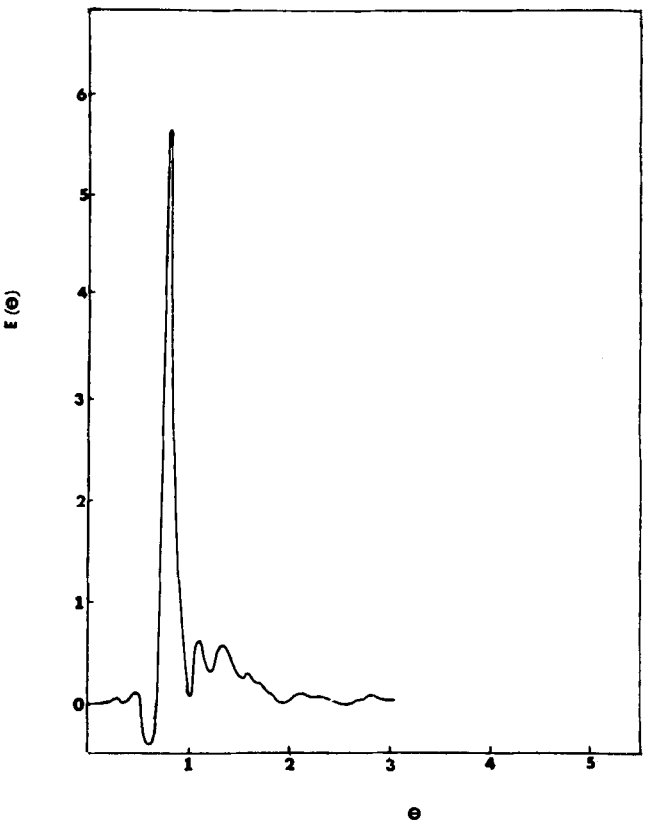

Fig. 7. Deconvoluted liquid phase residence time distribution.

The improvement of the fit when Labrecque's correlation is used is clear from visual inspection of Figure 4 and is confirmed by the calculated correlation coefficient $R = 0.965$. This agreement between theoretical prediction and experimental data suggests the appropriateness of the model for the pulp slurry used in this study and validates two assumptions in particular: the representation of interphase drag by Darcy's law and the applicability of the Kozeny-Carman equation for the viscous flow resistance.

The values of the empirical coefficients obtained by Labrecque with flexible nylon fibers are not universally valid but rather should be determined for each specific material. The settling data obtained in this study were used to determine the coefficients for Labrecque's correlation by least-squares analysis, leading to the following equation for the Kozeny factor:

$$k = 7.82 - 11.05\epsilon + 9.48\epsilon^2 \qquad (33)$$

The resulting fit, which is shown in Figure 5, yields a correlation coefficient $R = 0.988$.

Tracer Responses

Tracer runs were performed both in the pipe and in the tower. In most of the runs, the water Reynolds number was less than 2 500; according to charts published by Bugliarello and Daily (1961), these runs should all fall in the laminar flow regime.

A representative response for liquid tagging in the pipe is shown in Figure 6. In the particular run shown, the amount of pulse overlapping was minimal; in some runs in the pipe, the overlap was more accentuated and in others it was much less, while in the tower, overlap was never a problem. Figure 7 shows the residence time distribution obtained by the deconvolution procedure outlined in the previous section. The shape of this pulse indicates a small amount of dispersion, and the symmetry of the

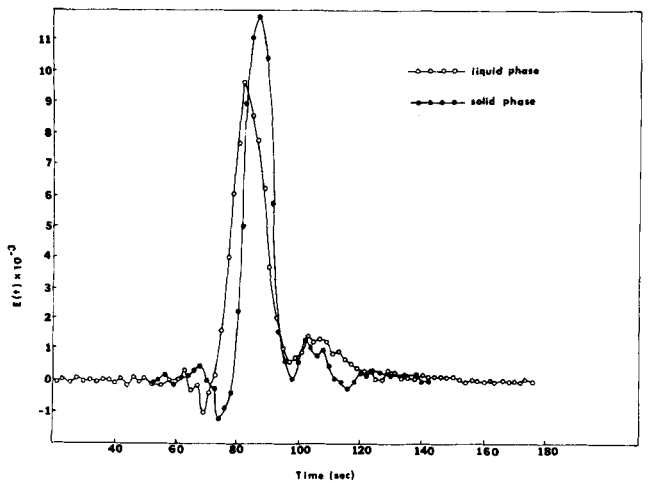

Fig. 8. Representative liquid and solid phase residence time distributions.

pulse indicates a much flatter velocity profile than would be encountered in laminar flow of a Newtonian fluid. The spurious oscillations in the tail of the pulse are characteristic Gibbs phenomena, caused by truncation of the Fourier transform prior to inversion.

In several pairs of successive runs in the pipe, the liquid and solid phases were tagged at nearly identical flow rates. (Limitations in the radiation detection system precluded the simultaneous tagging of both phases in a single run.) The volumetric flow rates during each run were measured gravimetrically, and the deconvoluted impulse responses were time scaled to a common flow rate.

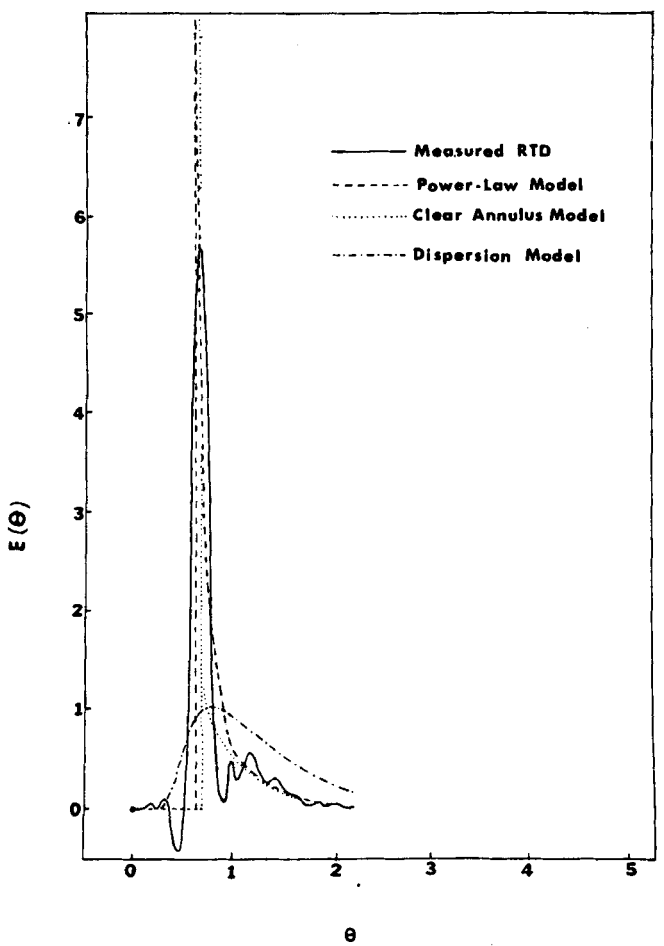

Fig. 10. Measured residence time distribution and three model responses.

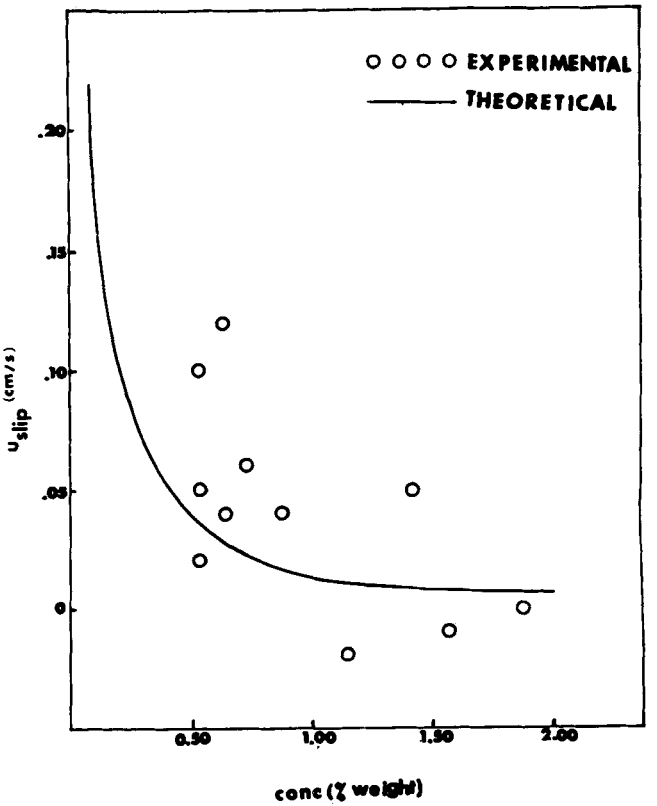

Fig. 9. Slip velocity vs. slurry consistency.

Typical scaled responses are shown in Figure 8. The mean residence times of each phase were determined from the peak response times (the symmetry of the peaks made this technique preferable to the more cumbersome method of moments), and the slip velocity was calculated from the difference in the residence times.

Interphase Slip Velocities

Slip velocities determined in the manner described in the preceding section are plotted against the slurry consistency in Figure 9. Also shown on this figure is the curve predicted by the Kozeny-Carman equation, Equation (21), with Equation (33) being used to predict the Kozeny factor. The data encompass all the runs in the pipe for

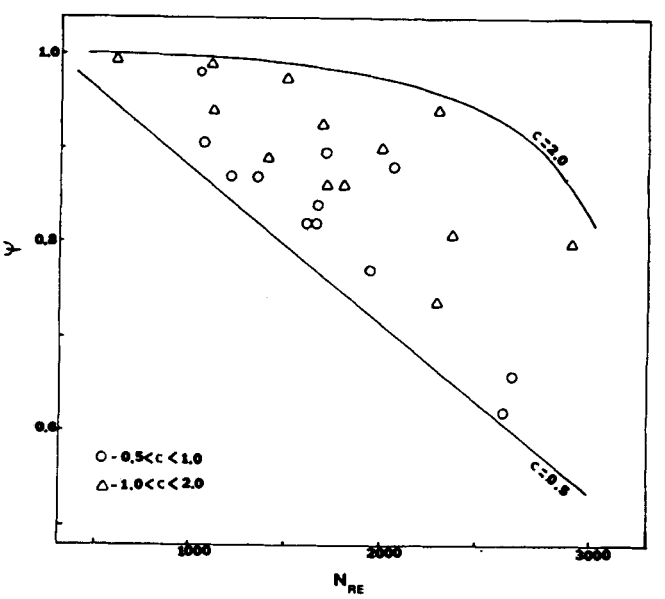

Fig. 11. Clear annulus model: normalized core radius vs. Reynolds number.

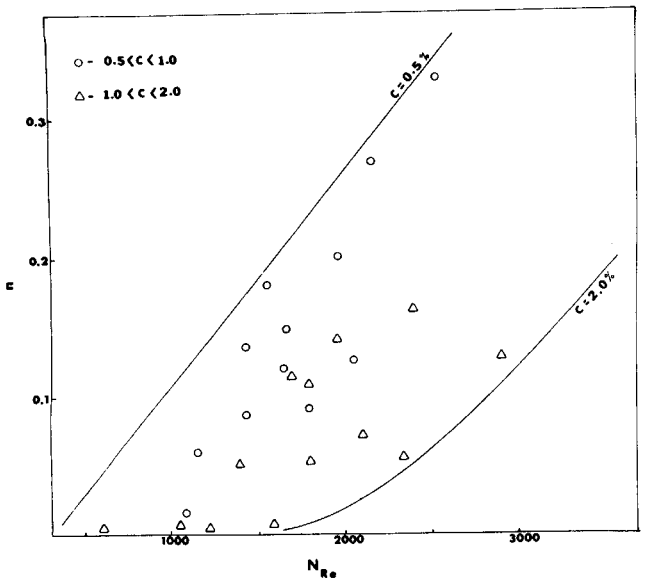

Fig. 12. Power law model: n vs. Reynolds number.

which the Reynolds number was less than 1 100, so that flow instabilities and pulse overlapping were not complicating factors. The scatter in the data is substantial, but no more could be expected in view of the low magnitudes of the slip velocities and approximations in the data analysis required to determine them. The trend predicted by the model can be clearly observed; however, the model appears to consistently underpredict the slip velocity, a point to which we will subsequently return.

The greatest deviations between experiment and theory appearing in Figure 9 are at the lower pulp consistencies, below about 0.5 wt%. Two factors other than random measurement errors could be responsible in part for these deviations: failure of the tagged glass fibers to follow precisely the same flow pattern as the pulp which forms the bulk solid phase, and departure from a uniform velocity profile. Both of these phenomena are known to become less significant at higher slurry consistencies, where the pulp fiber forms a more continuous phase and entrains the glass fibers, and the velocity profile becomes quite flat over most of the flow channel cross section, even in laminar flow.

Deviations resulting from errors in the measurement of the pulp parameters, especially in the density of the swollen fibers, are not likely to be of great significance, as indicated by the good agreement obtained in the settling tests previously described.

Liquid Phase Residence Time Distributions

Figure 10 shows a representative deconvoluted residence time distribution for liquid tagging in a pipe run, along with the best fitted responses for the clear annulus and power law models. Also shown is the response predicted by fitting the axial dispersion model to the experimental data.

It is apparent that both laminar flow models provide a far more accurate representation of the behavior of the system than does the dispersion model. It is difficult to choose between the clear annulus and power law models on the basis of goodness of fit; both models qualitatively simulate the experimental response, but the data points show a degree of axial dispersion about the mean which cannot be represented by either model. The spread of the experimental distribution may be attributable in part to imperfect collimation of the response peaks, but it is more likely a consequence of two contraventions of several assumptions inherent in the models, specifically, a flat core

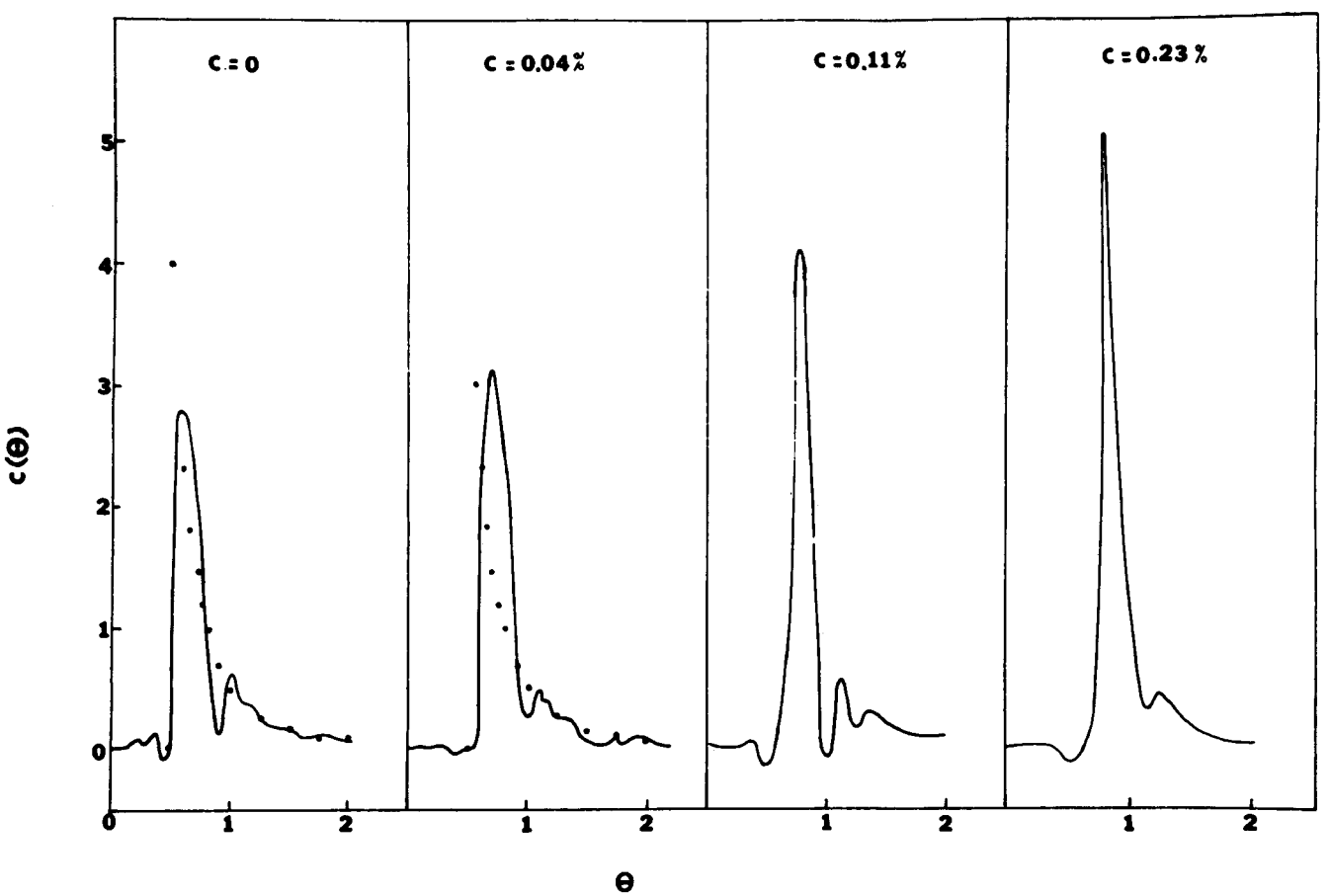

Fig. 13. Residence time distributions for four slurry consistencies.

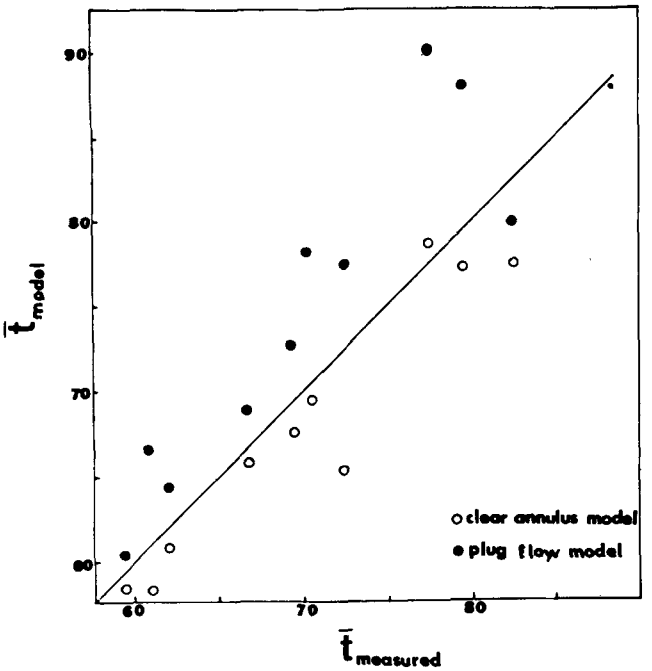

Fig. 14. Predicted vs. measured solid phase mean residence time.

velocity in the clear annulus model and the neglect of dispersion due to interphase slip or local turbulent mixing in both models.

A more accurate representation of the residence time distribution would require analysis of the full two phase model outlined previously, an extremely complex task. The task may not be justified, however; the clear annulus model has been reasonably successful at correlating the hydrodynamic behavior of slurries, and the disparities between the measured and model residence time distributions shown in Figure 10 may not have a significant effect on predicted conversion levels if the solid phase is undergoing a chemical reaction. (This point is discussed further in a subsequent section.)

The residence time distributions obtained in the liquid tagged runs performed on the pipe and tower were fit with both the clear annulus and power law models. Figure 11

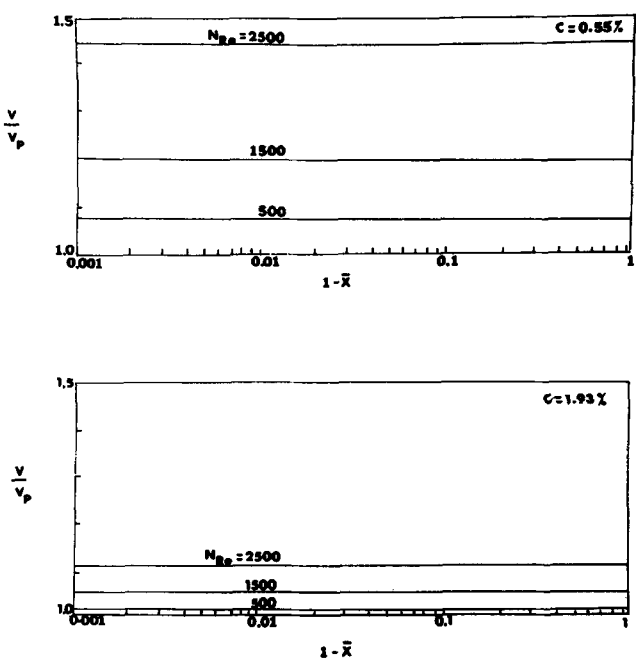

Fig. 15. Effects of phase segregation on reactor design.

shows a plot of $(R_c/R_t)^2$ vs. Reynolds number. The results are scattered, but the pattern is clear: the effective core radius approaches the pipe radius at low Reynolds numbers and high slurry consistencies and decreases as N_{Re} increases and c decreases.

Figure 12 shows a similar plot for the parameter n of the power law model [Equation (1)], which is seen to vary over a broad range but to follow a distinct pattern of variation with N_{Re} and c.

Several researchers have performed studies of very low concentration suspensions. Forgacs et al. (1958) observed that when consistencies are below 0.01%, the fibers are sufficiently separated from one another to undergo only occasional collisions, while at consistencies upwards of 0.05%, interactions play an increasingly important role. Bugliarello and Daily (1961) note that below 0.20%, the amount of counterrotation decreases sharply, indicating that the network is not continuous at such concentrations.

The results of the present studies also indicate that even when the pulp suspension becomes highly dilute, the flow deviates considerably from the pattern characteristic of a Newtonian fluid in laminar flow. To further verify this result, runs were carried out in the pipe with pure water and for slurry concentrations of 0.04, 0.11, and 0.23%. The resulting residence time distributions, which are plotted in Figure 13, show the pronounced effect of a low fiber concentration on the velocity profile.

Solid Phase Residence Time Distributions

The residence time distribution of the solid phase of a slurry in vertical laminar flow may be obtained by superimposing a uniform slip velocity on one of the liquid phase RTD models outlined above. For its simplicity and the fact that it embodies, at least qualitatively, observed hydrodynamic characteristics of slurry flow, we have chosen the clear annulus model as a basis. The solid is therefore taken to be moving in plug flow in a core of radius R_c. The core radius is first estimated from the correlation curves of Figure 11; the liquid core velocity u_{lm} is next determined from Equation (10), the slip velocity u_{slip} is calculated from Equation (21), and finally the solid phase velocity is determined as $u_{lm} - u_{slip}$. The residence time distribution of the solid is, according to this model, a delta function at $t_o = L/u_s$.

Figure 14 shows plots of the mean residence time of the solid phase predicted by this model vs. the measured value; also plotted are the values which would be predicted if the simple assumptions of uniform plug flow and no slip were made. The residence times predicted by the clear annulus-slip flow model are seen to be lower than the measured values, probably reflecting both the underprediction of slip velocities illustrated in Figure 9 and the broad range of possible values of the core radius R_c shown in Figure 11. Nevertheless, the correspondence of the measured and predicted values is closer than would be obtained if the simple ideal plug flow model were assumed; moreover, the model assumption of a central plug and a clear annulus is consistent with visual observations of laminar slurry flows. For these reasons, the clear annulus model with slip should be regarded as preferable for reactor modeling.

Illustrative Reactor Modeling Calculations

For illustrative purposes, effects of the slurry flow patterns described above on the performance of a chemical reactor have been estimated. A second-order reaction between the solid and a constituent of the liquid was postulated. (The bleaching reaction between dissolved chlorine and lignin in pulp is an example of such a reaction.) The

ratio of the volume required to achieve a specified fractional conversion to the volume of an ideal plug flow reactor required for the same conversion was calculated.

Since the radial nonuniformity of the velocity profile in the flow channel increases with increasing Reynolds number and decreasing slurry consistency, the volume ratio should exhibit the same trend. That it does so is confirmed by plots shown in Figure 15.

ACKNOWLEDGMENT

A paper based on this work was presented at the 69th Annual Meeting of the AIChE, Chicago, Illinois, November, 1976. The authors acknowledge with gratitude the fellowship support provided by the Brazilian Nuclear Energy Commission.

NOTATION

A = cross-sectional area of pulp bed in permeability cell, cm^2
A_r = aspect ratio of fibers
a_n = parameter in Labrecque's correlation, Equation (25)
b_n = parameter in Labrecque's correlation, Equation (25)
c = mass concentration of fiber in dispersion, g/cm^3
c_n = parameter in Labrecque's correlation, Equation (25)
E = residence time distribution, s^{-1}
Ei = exponential integral $\left[= \int_1^\infty (e^{-3t}/t^n)dt \right]$
$E(t)$ = residence time distribution in test section
F = drag force exerted by liquid phase on a suspended solid particle, dynes
$\overline{F}$ = resultant force exerted by fluid on particles per unit volume of mixture, dynes/cm^3
G = Laplace transform of $E(t)$
g = acceleration of gravity, cm/s^2
H = unit step function
K = permeability coefficient of a porous bed, cm^2
k = Kozeny factor
L = reactor length; porous bed depth, cm
m = parameter of power law model
N = total number of samples
N_{Re} = Reynolds number
n = parameter of power law model
p = pressure, dynes/cm^2
Q = volumetric flow rate, cm^3/s
R = correlation coefficient
R_c = radius of core in clear-annulus model (cm)
Re = real part of a complex number
R_t = cylindrical conduit radius, cm
r = radial position coordinate, cm
S_p = particle surface-to-volume ratio, cm^{-1}
s = Laplace transform variable
t = time, s
$\overline{t}$ = nominal mean residence time, s
t_o = breakthrough time, s
U = unit step function
u = linear velocity, cm/s
$\overline{u}$ = mean velocity, cm/s
u_l = velocity of liquid phase, cm/s
u_{lm} = maximum (central core) velocity, cm/s
u_m = maximum velocity (at center of cross section)
u_s = velocity of solid phase, cm/s
u_{slip} = slip velocity, $u_{lm} - u_s$, cm/s
V = volume of solid particle in suspension, cm^3
$\overline{V}$ = specific volume of fibers, cm^3/g
v_s = predicted value of fiber settling velocity, cm/s
v_{si} = measured value of fiber settling velocity, cm/s
$\overline{v_s}$ = average value of v_s, cm/s
W = Whittaker's function
z = distance variable, cm

Greek Letters

Γ = Gamma function
δ = delta function
Δp = pressure drop across bed
ϵ = fractional volume occupied by liquid phase in a slurry
κ = permeability of pulp to liquid
θ = $t/\overline{t}$, dimensionless time
μ = viscosity of fluid phase (poise)
ν = $(n+1)/(n-1)$, a parameter in Whittaker's equation, Equation (7)
ρ_l = density of liquid phase, g/cm^3
ρ_f = density of dry paper pulp fibers, g/cm^3
ρ_s = density of wet paper pulp fibers, g/cm^3
σ = specific surface of fibers, cm^3/g
τ = shear stress, dynes/cm^2
τ_{rz} = rz component of viscous stress tensor, dynes/cm^2
τ_o = yield stress, dynes/cm^2
ψ = R_c/R_t

Operators

D = substantial derivative
∇ = gradient vector
$\nabla\cdot$ = divergence

LITERATURE CITED

Ackroyd, M. H., *Digital Filters*, Butterworths, London, England (1973).

Balla, B., P. Fejes, L. Kalman, and A. Sarkany, "Untersuchung von Stoffstromen in den Stoffauflauf Kasten der Papierindustrie mit der Markierungstechnik," *Isotopenpraxis*, 6, 224 (1971).

Beek, W. J., H. J. de Ridder, J. P. W. Houtman, and W. Kuiper, "Residence Time Distributions in Laminar Flow and During the Passage of Granular Solids Through Rotary Kilns," in *Radioisotope Tracers in Industry and Geophysics*, (Proceedings Symposium, Prague, 1966), pp. 537-549, I.A.E.A., Vienna (1967).

Bird, B. B., W. E. Stewart, and E. N. Lightfoot, *Transport Phenomena*, Wiley, New York (1965).

Bosworth, R. C. L., "Distribution of Reaction Times for Laminar Flow in Cylindrical Reactors," *Phil. Mag.*, 39, 847 (1948).

Brecht, W., and H. Heller, "A Study of the Pipe Friction Losses of Paper Stock Suspensions," *TAPPI*, 33, 14A (1950).

Brigham, E. O., *The Fast Fourier Transform*, Prentice-Hall, Englewood Cliffs, N.J. (1974).

Broadkey, R. S., *The Phenomena of Fluid Motion*, Addison-Wesley, Reading, Mass. (1967).

Bugliarello, G., and J. W. Daily, "Rheological Models and Laminar Shear Flow of Fiber Suspensions," *TAPPI*, 44, 881 (1961).

Chatters, R. M., and R. L. Petterson, "Use of Tracers in In-Plant Evaluation of Processes and in Pollution Control of Effluent from Pulp and Paper Mills into Rivers," in *Radioisotope Tracers in Industry and Geophysics* (Proceedings Symposium, Prague, 1966), pp. 251-258, I.A.E.A., Vienna 1967).

———, "Paper Mill Fiber and Chip Tagging and Tracing Technique," in R. D. Rice College of Engineering-Research Division, *Bulletin 312* (RLO-1951-1), Washington State Univ. (1969).

Cowan, W. F., "Wet Pulp Characterization by Means of Specific Surface, Specific Volume and Compressibility," *Pulp Paper Mag. Canada*, 71, No. 9, 63 (1970).

Daily, J. W., and G. Bugliarello, "A Particulate Non-Newtonian Flow," *Ind. Eng. Chem.*, 51, 887 (1959).

———, "Basic Data for Dilute Fiber Suspensions in Uniform Flow with Shear," *TAPPI*, 44, 497 (1961).

Emmons, H. W., "The Continuum Properties of Fiber Suspensions," *ibid.*, **48**, 679 (1965).
Fan, L. T., and W. S. Hwang, "Dispersion of Ostwald-de Waele Fluid in Laminar Flow Through a Cylindrical Tube," *Proc. Roy. Soc. (London)*, **A283**, 576 (1965).
Fogelberg, B. C., and M. Johanson, "The Use of Radioactive Tracers in Investigations into Bleaching Process," *Paperi ja Puu*, **40**, 571 (1958).
Forgacs, O. L., A. A. Robertson, and S. G. Mason, "The Hydrodynamic Behaviour of Paper-Making Fibres," *Pulp Paper Mag. Canada*, **59**, No. 5, 117 (1958).
Gardner, R. P., R. M. Felder, and T. S. Dunn, "Tracer Concentration Responses and Moments for Measurements of Laminar Flow in Circular Tubes," *Intern. J. Appl. Rad. Isotopes*, **24**, 235 (1973).
Han, T. S., "The Status of the Sheet Forming Process—A Critical Review," *Inst. Paper Chemi.*, Appleton, Wisc. (1965).
Harrison, R. E., R. M. Felder, and R. W. Rousseau, "Accuracy of Parameter Estimation by Frequency Response Analysis," *Ind. Eng. Chem. Process Design Develop.*, **13**, 389 (1974).
Labrecque, R. P., "The Effects of Fiber Cross Sectional Shape on the Resistance to the Flow of Fluids Through Fiber Mats," *TAPPI*, **51** (1968).
Letan, R., "On Vertical Dispersed Two-Phase Flow," *Chem. Eng. Sci.*, **29**, 621 (1974).
Levenspiel, O., and J. C. R. Turner, "The Interpretation of Residence-Time Experiments," *ibid.*, **25**, 1605 (1970).
Levenspiel, O., B. W. Lai, and C. Y. Chatlynne, "Tracer Curves and the Residence Time Distribution," *ibid.*, 1611 (1970).
Ljunggren, K., "Review of the Application of Radioactive Tracers in the Pulp and Paper Industry," in *Radioisotopes in the Pulp and Paper Industry* (Proceedings Panel Helsinki, 1967), pp. 39-51, I.A.E.A., Vienna (1968).
Mason, S. G., and R. St. J. Manley, "Fiber Motions and Flocculation," *TAPPI*, **37**, 494 (1952).
Metzner, A. B., "Non-Newtonian Technology: Fluid Mechanics, Mixing and Heat Transfer," *Advan. Chem. Eng.*, **1**, 77 (1956).
Mih, W., and J. Parker, "Velocity Profile Measurements and a Phenomenological Description of Turbulent Fiber Suspension Pipe Flow," *TAPPI*, **50**, 237 (1967).
Moller, K., G. G. Duffy, and A. L. Titchener, "The Laminar Plug Flow Regime of Paper Pulp Suspensions in Pipes," in *Svensk Papperstidning*, **74**, 829 (1971).
Moller, K., and G. G. Duffy, "Plug Flow of Pulp Suspensions: Comment," *TAPPI*, **57**, 123 (1974).
Moreira, R. M., "Dynamic Modeling of Paper Pulp Slurry Flow Using Radiotracers," Ph.D. thesis, N.C. State Univ., Raleigh (1976).
Nelson, R. W., "Approximate Theories of Filtration and Retention," *TAPPI*, **47**, 752 (1964).
Novosad, Z., and J. Ulbrecht, "Conversion in Chemical Reactions for Isothermal Laminar Flow of Non-Newtonian Liquids in a Tubular Reactor of Circular Cross-Section," *Chem. Eng. Sci.*, **21**, 405 (1965).
Osborne, F. T., "Purely Convective Models for Tubular Reactors with Non-Newtonian Flow," *ibid.*, **30**, 159 (1975).
Robertson, A. A., and S. G. Mason, "Specific Surface of Cellulose Fibers by the Liquid Permeability Method," *Pulp Paper Mag. Canada*, **50**, No. 12, 103 (1949).
Robertson, A. A., "Flow of Dilute Fiber Suspensions," *TAPPI*, **48**, 98A (1965).
Sanders, H. T., Jr., and H. Meyer, "Consistency Distributions in Turbulent Tube Flow of Fiber Suspensions," *ibid.*, **54**, 722 (1971).
Sankey, C. A., S. G. Mason, G. A. Allen, and W. R. Keating, "Application of Radioactive Tracers to Measurements of Fibre Flow and Distribution," *Pulp Paper Mag. Canada*, **52**, No. 3, 136 (1951).
Schweitzer, G., "Studie zur Kennzeichung von Papierfaserstoffen durch ihre Spezifische Oberflache," *Das Papier*, **29**, 9 (1975).
Sheppard, C. W., M. P. Jones, and B. L. Couch, "Effect of Catheter Sampling on the Shape of Indicator-Dilution Curves," *Circulation Res.*, **7**, 895 (1959).
Stamm, A. J., "Density of Wood Substance, Adsorption by Wood, and Permeability of Wood," *J. Phys. Chem.*, **33**, 398 (1929).
Stenuf, T. J., and K. P. Anumolu, "Plug Flow of Pulp Suspensions," *TAPPI*, **55**, 1387 (1972).
Wein, O., and J. Ulbrecht, "Residence Time Distribution in Laminar Flow Systems. II—Non-Newtonian Tubular Flow," *Collection Czechoslov. Chem. Commun.*, **37**, 3240 (1972).
Wen, C. J., and L. T. Fan, *Models for Flow Systems and Chemical Reactors*, Marcel Dekker, New York (1975).
Wrist, P. E., "Flow Properties of Fibrous Suspensions," in *Surfaces and Coatings Related to Paper and Wood*, by R. H. Merchessault, and C. Skaar, eds., Syracuse University Press, Syracuse, N.Y. (1967).
Zuber, N., "On the Dispersed Two-Phase Flow in the Laminar Flow Regime," *Chem. Eng. Sci.*, **19**, 897 (1964).

Manuscript received January 23, 1978; revision received August 25, and accepted September 6, 1978.

Dynamic Response of the Carbon Dioxide Electrode

TERRENCE L. DONALDSON

and

HARVEY J. PALMER

Department of Chemical Engineering
University of Rochester
Rochester, New York 14627

Complex relationships among multiple chemical species during unsteady diffusion and reaction are shown to cause hysteresis, *p*H dependent response rates, and general nonfirst-order transient behavior in agreement with common experimental observations. Response improvement by enzymic catalysis of the carbon dioxide hydration reaction also is considered.

SCOPE

Potentiometric electrodes have become common analytical devices. Although their equilibrium behavior is reasonably well understood, their transient behavior is poorly characterized, and they often exhibit nonideal phenomena. An example is the carbon dioxide electrode (Stow, Baer, and Randall, 1957), which is an adaptation of the common glass membrane *p*H electrode in which the *p*H of a thin layer of bicarbonate solution in equilibrium with ambient carbon dioxide is measured. It is used routinely in blood gas analysis, in vivo blood studies, and respiratory gas analysis.

Correspondence concerning this paper should be addressed to Terrence L. Donaldson.